引用格式：XIA Hongming, ZHANG Duo, LI Yaqian, et al. Two-dimensional Electromagnetically Induced Grating in Microwave Coupled Four-level Atomic System[J]. Acta Photonica Sinica, 2023, 52(1):0105002
夏红铭,张多,李亚骞,等.微波耦合四能级原子系统二维电磁感应光栅[J].光子学报,2023,52(1):0105002

微波耦合四能级原子系统二维电磁感应光栅

夏红铭,张多,李亚骞,孙照宇,王梅
(武汉轻工大学 电气与电子工程学院, 武汉 430023)

摘　要:提出一种利用微波场在四能级原子系统中实现二维电磁感应光栅的理论研究方案,此原子系统中两个偶极禁戒的亚稳态之间采用微波场来耦合。分析了微波场存在与否对弱探测场夫琅禾费衍射图样的影响。讨论了有微波场存在时,探测场失谐量、控制场强度、相互作用长度等对二维电磁感应光栅衍射效率的影响。结果表明,通过合适地调节系统参数,在所研究的系统中可以实现高衍射效率的二维电磁感应光栅。该方案可应用于全光分束和光开关,对光信息处理及光网络通信研究有一定帮助。

关键词:电磁感应光栅;微波场;相位调制;衍射效率;驻波激光场
中图分类号:O431.2　　**文献标识码**:A　　**doi**:10.3788/gzxb20235201.0105002

0　引言

近年来,光场与原子系统之间相互作用的一些物理现象,如:相干布居俘获(Coherent Population Trapping, CPT)[1]、电磁感应透明(Electromagnetically Induced Transparency, EIT)[2]、自发辐射相干(Spontaneously Generated Coherence, SGC)[3]等引起了人们的广泛关注,其中基于EIT的电磁感应光栅(Electromagnetically Induced Grating, EIG)现象成为近些年的研究热点。在EIT效应中,强的行波耦合场与原子间量子相干使得介质对弱的探测光零吸收。如果把行波场替换为具有空间调制形式的驻波场,则可交替出现高透射区和吸收区,介质对探测光的吸收和色散等性质也会相应的受到空间调制,入射的探测光经过该驻波调制的区域后将被衍射,这样原子介质就形成了类似光栅的结构,这种现象被称为EIG。EIG克服了传统光栅的很多局限性,对振幅和相位可以同时进行调制,其光栅常数、衍射光能量和衍射级次可以通过改变驻波场的波长以及入射光场的强度和失谐量进行调控。由于其具备诸多优势,EIG已引起人们的广泛关注,并被应用于全光开关和路由[4]、相干诱导光子带隙[5]、量子Talbot效应[6]、分束器[7]等光量子器件的研究领域中。

EIG这一概念最早是在三能级Λ型原子系统[8]的理论研究上提出的。随后,研究者们先后在冷原子系统[9]和热原子系统[10]的实验上观察并研究了EIG效应。DUTTA B K等[11]研究了在共振和非共振双光子吸收条件下,三能级Ξ型原子系统的EIG特性;XIAO Z H团队[12]研究了双暗态下微波场耦合原子系统的电磁感应相位光栅的衍射效率;文献[13]报道了在EIT条件下,增强交叉Kerr非线性可以得到类似理想正弦位相光栅的电磁感应位相光栅;基于Fano干涉和光子诱导效应,关于EIG的研究扩展到非对称半导体量子阱[14]和量子点系统[15-17]中。此外,为了抑制线性吸收且获得更高的衍射效率,在其他量子系统中一些EIG的理论和实验方案[18-23]也被提出。近年来,EIG的研究逐渐向二维空间发展,WANG L等[24]利用两个正交的驻波场,在三角架型四能级原子系统中实现了二维电磁感应交叉光栅,结果表明,一阶衍射强度明显取决于探测场失谐和耦合驻波场的拉比频率。WU J C等[25]和CHENG G L等[26]分别在N型原子系统和二能级原

基金项目:国家自然科学基金(Nos.11675124, 12105210),武汉轻工大学校立科研项目(No. 2021Y36)
第一作者:夏红铭,XHM_xiahongming@163.com
通讯作者:张多,zhangduo10@126.com
收稿日期:2022-06-14;**录用日期**:2022-07-14

子系统中研究了二维EIG效应。为了进一步调节衍射级次和提高衍射效率，WANRG研究小组[27-29]提出几种有趣的方案实现了位相光栅和增益位相光栅。此外，P-T对称性[30-31]、Raman相互作用[32]、涡旋场的方位调制[33]等也被用来实现高效率的二维EIG。

本文提出在双暗态的四能级原子系统中研究二维电磁感应光栅效应。在该原子系统中两个超精细结构，偶极禁戒的亚稳态之间采用微波场来耦合。由于微波场的存在，会引发两种不同的暗共振，通过合适地调节微波场强度，可以同时实现低吸收和高折射[34-36]，使原子响应得到有效控制，有利于提高光栅的衍射效率。而且，本文提出的方案能级结构比较简单，在微波场的作用下，通过调节系统参数，如探测场失谐量、驻波耦合场强度、相互作用长度等可以实现高衍射效率的二维EIG。

1 理论模型与动力学方程

如图1(a)，考虑一个辅助的微波场耦合的四能级原子系统，该系统由一个激发态$|4\rangle$和两个亚稳态$|2\rangle$、$|3\rangle$以及一个低能态$|1\rangle$组成。用拉比频率为$\Omega_p=\mu_{41}E_p/2\hbar$的弱探测场来耦合跃迁$|1\rangle\rightarrow|4\rangle$，强度在空间上周期性变化的二维驻波耦合场$\Omega_c=\Omega\left[\sin\left(\pi x/\Lambda_x\right)+\sin\left(\pi y/\Lambda_y\right)\right]$来驱动跃迁$|3\rangle\rightarrow|4\rangle$。该二维驻波耦合场由分别在$x$和$y$两个方向传播的驻波激光场所组成，其拉比频率为$\Omega=\mu_{43}E_c/2\hbar$，$\Lambda_x$和$\Lambda_y$为驻波的空间周期。其中亚稳态$|2\rangle$和$|3\rangle$是两个超精细能级，在偶极近似下$|2\rangle\rightarrow|3\rangle$能级跃迁是被禁止的。可以用一个拉莫频率为$\Omega_m=\mu_{32}E_m/2\hbar$的辅助微波场用来驱动，其中$\mu_{ij}$表示跃迁能级$|i\rangle\rightarrow\left|j\right\rangle$之间的原子跃迁的偶极矩阵元，$E_i(i=p,c,m)$表示相应场的振幅。相应光场及微波场与原子跃迁的频率失谐定义为：$\Delta_p=\omega_{41}-\omega_p$、$\Delta_c=\omega_{43}-\omega_c$、$\Delta_m=\omega_{32}-\omega_m$，其中$\omega_{ij}$为原子能级$|i\rangle\rightarrow\left|j\right\rangle$之间的跃迁共振频率，$\omega_p$、$\omega_c$、$\omega_m$为相应光场及微波场的频率。探测场、耦合场以及微波场与原子系统相互作用空间结构关系如图1(b)，探测场E_p和微波场E_m沿z轴方向传播，耦合场E_c传播方向与z轴成一个小角度在与原子相互作用区域叠加从而形成驻波场。

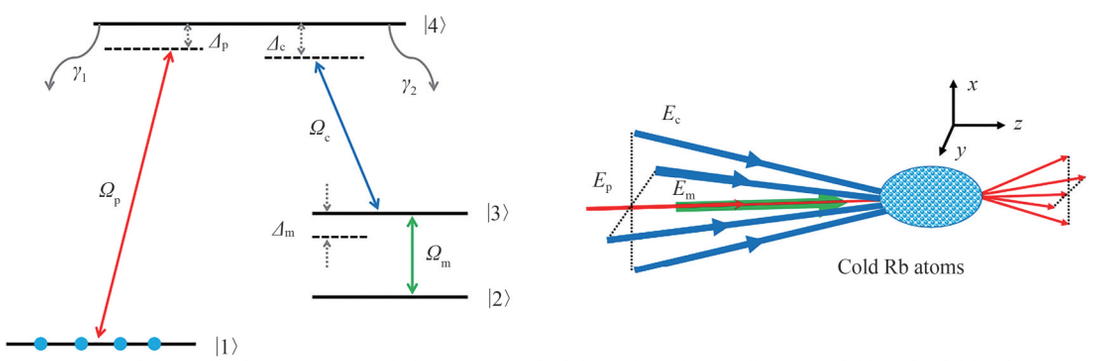

(a) Schematic of microwave coupled four level atomic system

(b) Schematic of the standing wave field, probe field and microwave field propagating through a cold atomic sample

图1 微波耦合四能级原子系统及与光场相互作用空间结构关系

Fig. 1 Schematic of microwave coupled four level atomic system and the schematic sketch of the spatial configuration of laser fields

根据光与物质相互作用的半经典理论，采用电偶极近似和旋波近似[37]，可以得到该系统相互作用的哈密顿量(设$\hbar=1$)，可表示为

$$\hat{H}_I=\Delta_p|4\rangle\langle4|+(\Delta_p-\Delta_c)|3\rangle\langle3|+(\Delta_p-\Delta_c+\Delta_m)|2\rangle\langle2|-\left[\Omega_p|4\rangle\langle1|+\Omega_c|4\rangle\langle3|+\Omega_m|3\rangle\langle2|+\text{H.c.}\right] \tag{1}$$

式中，H.c.表示厄密共轭项，考虑系统的弛豫过程，根据光与原子相互作用系统的密度算符运动方程(Liouville方程)，利用密度矩阵方法可得密度算符运动方程为

$$\begin{cases}\dot{\rho}_{44}=-\left(\gamma_1+\gamma_2\right)\rho_{44}+\mathrm{i}\Omega_{\mathrm{p}}\rho_{14}-\mathrm{i}\Omega_{\mathrm{p}}^{*}\rho_{41}+\mathrm{i}\Omega_{\mathrm{c}}\rho_{34}-\mathrm{i}\Omega_{\mathrm{c}}^{*}\rho_{43}\\ \dot{\rho}_{33}=\gamma_2\rho_{44}+\mathrm{i}\Omega_{\mathrm{m}}\rho_{23}-\mathrm{i}\Omega_{\mathrm{m}}^{*}\rho_{32}+\mathrm{i}\Omega_{\mathrm{c}}^{*}\rho_{43}-\mathrm{i}\Omega_{\mathrm{c}}\rho_{34}\\ \dot{\rho}_{22}=\mathrm{i}\Omega_{\mathrm{m}}^{*}\rho_{32}-\mathrm{i}\Omega_{\mathrm{m}}\rho_{23}\\ \dot{\rho}_{11}=\gamma_1\rho_{44}+\mathrm{i}\Omega_{\mathrm{p}}^{*}\rho_{41}-\mathrm{i}\Omega_{\mathrm{p}}\rho_{14}\\ \dot{\rho}_{43}=(-\mathrm{i}\Delta_{\mathrm{c}}-\gamma_{43})\rho_{43}-\mathrm{i}\Omega_{\mathrm{c}}\rho_{44}+\mathrm{i}\Omega_{\mathrm{c}}\rho_{33}-\mathrm{i}\Omega_{\mathrm{m}}^{*}\rho_{42}+\mathrm{i}\Omega_{\mathrm{p}}\rho_{13}\\ \dot{\rho}_{42}=[-\mathrm{i}(\Delta_{\mathrm{c}}+\Delta_{\mathrm{m}})-\gamma_{42}]\rho_{42}-\mathrm{i}\Omega_{\mathrm{m}}\rho_{43}+\mathrm{i}\Omega_{\mathrm{c}}\rho_{32}+\mathrm{i}\Omega_{\mathrm{p}}\rho_{12}\\ \dot{\rho}_{41}=(-\mathrm{i}\Delta_{\mathrm{p}}-\gamma_{41})\rho_{41}+\mathrm{i}\Omega_{\mathrm{p}}(\rho_{11}-\rho_{44})+\mathrm{i}\Omega_{\mathrm{c}}\rho_{31}\\ \dot{\rho}_{32}=(-\mathrm{i}\Delta_{\mathrm{m}}-\gamma_{32})\rho_{32}+\mathrm{i}\Omega_{\mathrm{m}}(\rho_{22}-\rho_{33})+\mathrm{i}\Omega_{\mathrm{c}}^{*}\rho_{42}\\ \dot{\rho}_{31}=[-\mathrm{i}(\Delta_{\mathrm{p}}-\Delta_{\mathrm{c}})-\gamma_{31}]\rho_{31}-\mathrm{i}\Omega_{\mathrm{p}}\rho_{34}+\mathrm{i}\Omega_{\mathrm{c}}^{*}\rho_{41}+\mathrm{i}\Omega_{\mathrm{m}}\rho_{21}\\ \dot{\rho}_{21}=[-\mathrm{i}(\Delta_{\mathrm{p}}-\Delta_{\mathrm{c}}-\Delta_{\mathrm{m}})-\gamma_{21}]\rho_{21}-\mathrm{i}\Omega_{\mathrm{p}}\rho_{24}+\mathrm{i}\Omega_{\mathrm{m}}^{*}\rho_{31}\end{cases}\tag{2}$$

该系统中，密度算符满足关系：$\Sigma_{i=1}^{4}\rho_{ii}=1$、$\rho_{ij}=\rho_{ji}^{*}$。$\gamma_{ij}$表示原子跃迁能级$|i\rangle\leftrightarrow\langle j|$的退相干速率。在弱场近似及稳态下，对于零阶密度矩阵元有$\rho_{00}^{(0)}=1$，$\rho_{jk}^{(0)}=0(j\neq0,k\neq0)$，利用微扰法计算可以得到与探测场吸收和折射率相关的一阶密度矩阵元$\rho_{41}^{(1)}$，其表达式为

$$\rho_{41}^{(1)}=\mathrm{i}\Omega_{\mathrm{p}}\frac{|\Omega_{\mathrm{m}}|^2+\Gamma_{21}\Gamma_{31}}{\Gamma_{21}|\Omega_{\mathrm{c}}|^2+\Gamma_{41}|\Omega_{\mathrm{m}}|^2+\Gamma_{21}\Gamma_{31}\Gamma_{41}}\tag{3}$$

式中，$\Gamma_{41}=\gamma_{41}+\mathrm{i}\Delta_{\mathrm{p}}$，$\Gamma_{31}=\gamma_{31}+\mathrm{i}\left(\Delta_{\mathrm{p}}-\Delta_{\mathrm{c}}\right)$，$\Gamma_{21}=\gamma_{21}+\mathrm{i}\left(\Delta_{\mathrm{p}}-\Delta_{\mathrm{c}}-\Delta_{\mathrm{m}}\right)$，$\gamma_{41}=(\gamma_1+\gamma_2)/2=\Gamma/2=\gamma_1$，$\gamma_1$和$\gamma_2$分别表示原子能级$|4\rangle$到能级$|1\rangle$和$|3\rangle$的衰减率，$\gamma_{31}=\gamma_{21}=0.002\Gamma=0.004\gamma_1$，$\Gamma=2\gamma_1$。为简单起见，在数值计算中，所涉及到的耦合场拉比频率Ω，辅助微波场拉莫频率Ω_{m}、失谐量Δ_{p}，Δ_{c}，Δ_{m}，均以γ_1来度量，对^{87}Rb原子而言是MHz的量级[38]。

根据原子介质的极化强度：$P_{\mathrm{p}}=\varepsilon_0\chi_{\mathrm{p}}E_{\mathrm{p}}=N_0\mu_{14}\rho_{41}$，$E_{\mathrm{p}}$为探测场的电场强度，可以推导出弱探测场的线性极化率，表示为

$$\chi_{\mathrm{p}}\left(\Delta_{\mathrm{p}}\right)=\frac{N_0\mu_{14}}{\varepsilon_0E_{\mathrm{p}}}\rho_{41}^{(1)}=K\frac{\gamma_1\rho_{41}^{(1)}}{\Omega_{\mathrm{p}}}=K\bar{\rho}_{41}^{(1)}\tag{4}$$

式中，令$K=N_0|\mu_{41}|^2/2\hbar\varepsilon_0\gamma_1$，$\bar{\rho}_{41}^{(1)}=\rho_{41}^{(1)}\gamma_1/\Omega_{\mathrm{p}}$，$N_0$是介质的原子数密度，$\varepsilon_0$为真空中的介电常数。为了考察探测场通过驻波场区域时的夫琅禾费衍射强度和图样，需要利用麦克斯韦方程组来进行计算。因为探测场沿z轴方向传播，相应的场通过原子样品的示意图如图1(b)，在慢变包络近似和稳态情况下，探测场的传播方程可表示为

$$\frac{\partial E_{\mathrm{p}}}{\partial z}=\mathrm{i}\frac{\pi}{\lambda_{\mathrm{p}}}\chi_{\mathrm{p}}\left(\Delta_{\mathrm{p}}\right)E_{\mathrm{p}}\tag{5}$$

式中，λ_{p}为探测场的波长，定义$\zeta=2\hbar\varepsilon_0\lambda_{\mathrm{p}}\gamma_1/\pi N_0|\mu_{41}|^2$作为探测场沿原子介质传播方向$z$方向的单位，$\zeta$是该四能级原子系统中共振弱探测场在振幅吸收为$\mathrm{e}^{-1}$的传播距离。因此式(5)可简写为$\partial E_{\mathrm{p}}/\partial z=\mathrm{i}\bar{\rho}_{41}^{(1)}E_{\mathrm{p}}/\zeta$，令$\alpha=\mathrm{Im}(\chi)$，$\beta=\mathrm{Re}(\chi)$分别表示探测场的吸收和色散。通过对式(5)求解，可以得出探测场与原子介质在相互作用长度$z=L$处的透射函数为

$$T(x,y)=\mathrm{e}^{-\alpha L}\mathrm{e}^{\mathrm{i}\beta L}\tag{6}$$

由此可知透射函数的振幅调制和位相调制分别为

$$\left|T(x,y)\right|=\left|\mathrm{e}^{-\alpha L}\right|\tag{7}$$

$$\Phi(x,y)=\beta L/\pi\tag{8}$$

对透射函数作傅里叶变换，可以得到探测场的夫琅禾费衍射方程为

$$I_{\mathrm{p}}(\theta)=|E(\theta)|^2\frac{\sin^2\left(M\pi\Lambda_x\sin\theta_x/\lambda_{\mathrm{p}}\right)}{M^2\sin^2\left(\pi\Lambda_x\sin\theta_x/\lambda_{\mathrm{p}}\right)}\cdot\frac{\sin^2\left(N\pi\Lambda_y\sin\theta_y/\lambda_{\mathrm{p}}\right)}{N^2\sin^2\left(\pi\Lambda_y\sin\theta_y/\lambda_{\mathrm{p}}\right)}\tag{9}$$

式中，

$$E(\theta)=\int_0^1\int_0^1 T(x,y)\mathrm{e}^{-\mathrm{i}2\pi x\Lambda_x\sin\theta_x/\lambda_\mathrm{p}}\mathrm{e}^{-\mathrm{i}2\pi y\Lambda_y\sin\theta_y/\lambda_\mathrm{p}}\mathrm{d}x\mathrm{d}y \tag{10}$$

式(10)为单个空间周期探测场的夫琅禾费衍射，本文数值计算中衍射效率均采用无量纲处理，其大小均以$I_0=|E(\theta)|^2$为参考标准。θ_x和θ_y为探测场在z方向传播的衍射角在x和y方向上的分量，M和N为二维光栅的空间周期数。第(m, n)级衍射峰的方向由光栅方程$\sin\theta_x=m\lambda_\mathrm{p}/\Lambda_x$和$\sin\theta_y=n\lambda_\mathrm{p}/\Lambda_y$决定，由此可以计算出第(0,0)级、(1,0)级、(0,1)级和(1,1)级衍射峰的强度，分别表示为

$$I_\mathrm{p}\left(\theta_x^0,\theta_y^0\right)=\left|\int_0^1\mathrm{d}x\int_0^1 T(x,y)\mathrm{d}y\right|^2 \tag{11}$$

$$I_\mathrm{p}\left(\theta_x^1,\theta_y^0\right)=\left|\int_0^1\mathrm{e}^{-\mathrm{i}2\pi x}\mathrm{d}x\int_0^1 T(x,y)\mathrm{d}y\right|^2 \tag{12}$$

$$I_\mathrm{p}\left(\theta_x^0,\theta_y^1\right)=\left|\int_0^1 T(x,y)\mathrm{d}x\int_0^1\mathrm{e}^{-\mathrm{i}2\pi y}\mathrm{d}y\right|^2 \tag{13}$$

$$I_\mathrm{p}\left(\theta_x^1,\theta_y^1\right)=\left|\int_0^1\mathrm{e}^{-\mathrm{i}2\pi x}\mathrm{d}x\int_0^1\mathrm{e}^{-\mathrm{i}2\pi y}T(x,y)\mathrm{d}y\right|^2 \tag{14}$$

2 数值结果与讨论

根据第1节得到的表达式及相应的数值结果来分析和讨论，研究系统参数的改变对二维电磁感应光栅夫琅禾费衍射强度和衍射效率等的影响。微波场的引入，使得原先的Λ型原子系统变为微波耦合的四能级原子系统，系统结构的改变对振幅调制、位相调制、夫琅禾费衍射强度和衍射效率等都有影响，可以把入射光调制到特定的衍射方向上，提高二维电磁感应光栅的衍射效率。为方便起见，以无单位量纲呈现数值结果，以下数值计算均以γ_1为耦合场拉比频率、辅助微波场拉莫频率以及相应光场和微波场失谐量的度量标准。

首先考察微波场对衍射效率的影响，如图2(a)和(b)，分别绘制了存在微波场及不存在微波场的情况下探测场的夫琅禾费衍射强度随$\sin\theta_x$和$\sin\theta_y$变化的分布图。当不存在微波场时，探测场的能量基本集中在零级衍射峰上，几乎没有其他的探测场能量分散在高阶方向上；当存在微波场时，零级衍射峰上的能量明显降低，其零级中心主峰的强度只有0.3左右，其余一部分能量被衍射到四个位于$\left(\sin\theta_x=\pm0.25,\sin\theta_y=0\right)$和$\left(\sin\theta_x=0,\sin\theta_y=\pm0.25\right)$的(1,0)级和(0,1)级衍射峰上，其衍射效率达到4%左右，只有极少数的能量被分散到(1,1)级衍射峰上，(1,1)级衍射效率约为1%。由此可知，微波场的存在能够削弱零级衍射强度并增大一级衍射强度，明显提高一阶衍射效率。因此，对其他参数的研究都在有微波场的情况下进行。

由式(3)、(4)可知，衍射强度与介质的极化率有很大关系，为了更清晰地说明图2的物理机制，绘制了存

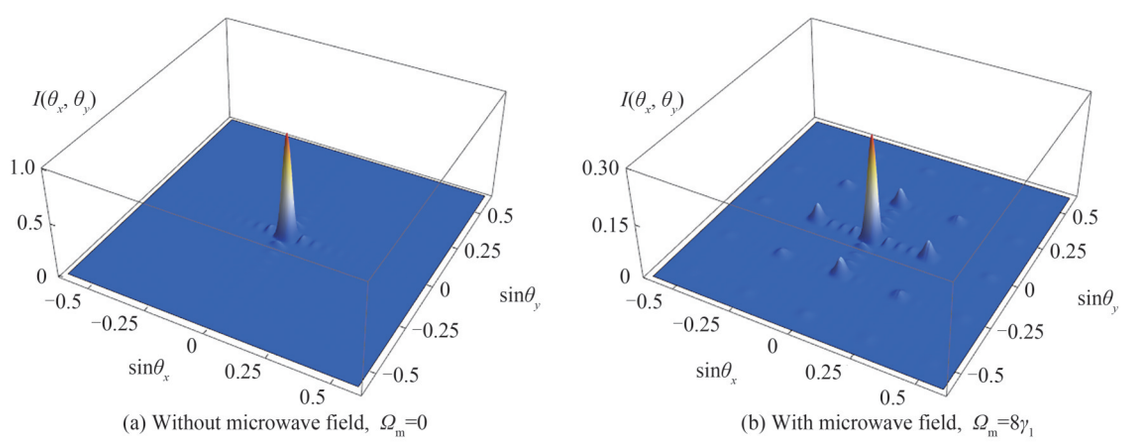

图2 夫琅禾费衍射强度随$\sin\theta_x$和$\sin\theta_y$变化分布($\Delta_\mathrm{p}=7\gamma_1$, $\Omega=8\gamma_1$, $L=8\zeta$, $\gamma_{21}=\gamma_{31}=0.004\gamma_1$, $\gamma_{41}=1$, $\Delta_\mathrm{c}=7\gamma_1$, $\Delta_\mathrm{m}=9.8\gamma_1$, $M=N=5$, $\Lambda_x=\Lambda_y=4\lambda_\mathrm{p}$)

Fig. 2 Fraunhofer diffraction intensity as a function of $\sin\theta_x$ and $\sin\theta_y$ ($\Delta_\mathrm{p}=7\gamma_1$, $\Omega=8\gamma_1$, $L=8\zeta$, $\gamma_{21}=\gamma_{31}=0.004\gamma_1$, $\gamma_{41}=1$, $\Delta_\mathrm{c}=7\gamma_1$, $\Delta_\mathrm{m}=9.8\gamma_1$, $M=N=5$, $\Lambda_x=\Lambda_y=4\lambda_\mathrm{p}$)

在微波场的情况下探测场极化率的实部 $\mathrm{Re}\left(\bar{\rho}_{41}^{(1)}\right)$（蓝色实线）和虚部 $\mathrm{Im}\left(\bar{\rho}_{41}^{(1)}\right)$（黄色虚线）随失谐量 Δ_p 的变化曲线（如图 3）。极化率的实部 $\mathrm{Re}\left(\bar{\rho}_{41}^{(1)}\right)$ 表示折射率或色散，由式(8)可以看出极化率的实部的正负影响位相调制深度。而极化率的虚部 $\mathrm{Im}\left(\bar{\rho}_{41}^{(1)}\right)$ 为正表示介质对探测光吸收，为零表示零吸收，也就是介质对探测光透明，为负表示增益。观察极化率虚部 $\mathrm{Im}\left(\bar{\rho}_{41}^{(1)}\right)$ 可以发现三个峰大概以 $10\gamma_1$ 间隔出现，表示该双暗态原子系统在三个强吸收峰之间出现两个电磁感应透明窗口，因为辅助微波场强度 Ω_m 以及失谐量等相关参数的调节，使得极化率的实部和虚部表现近周期性的变化。可以看到，在失谐量 Δ_p 处于 $-2\gamma_1\sim6\gamma_1$ 区间出现电磁感应透明窗口，介质对探测光表现为接近零吸收，折射率较为平缓地降低或增加。而失谐量在 $6\gamma_1\sim10\gamma_1$ 等区间时，折射率都比较高，先陡然上升再急剧下降，且失谐量在 $8\gamma_1$ 附近出现峰值，介质对探测光强烈吸收。在失谐量 $\Delta_\mathrm{p}=7\gamma_1$ 时，介质对探测光吸收较小，探测光基本可以透明传输，损失较小，而折射率却比较高，因此探测光在通过周期变化的驻波区域后将发生衍射，形成电磁感应光栅。接着，在图 4(a)和(b)中考察二维电磁感应光栅透射函数的振幅调制（$\left|T\left(x,y\right)\right|$）和位相调制（$\Phi\left(x,y\right)$）。在探测场失谐量 Δ_p 取 $7\gamma_1$，相互作用长度 L 取 8ζ 的情况下，振幅调制在平均透过率为 50% 附近上下振荡，这是由于通过微波场和耦合场的共同作用，介质的线性吸收受到抑制，有部分能量损耗。与此同时，驻波场的周期性变化使得透射函数的位相也发生周期性变化，位相调制深度达到了 2.6，表明在这种情况下，原子介质具有一定的相位调制能力。

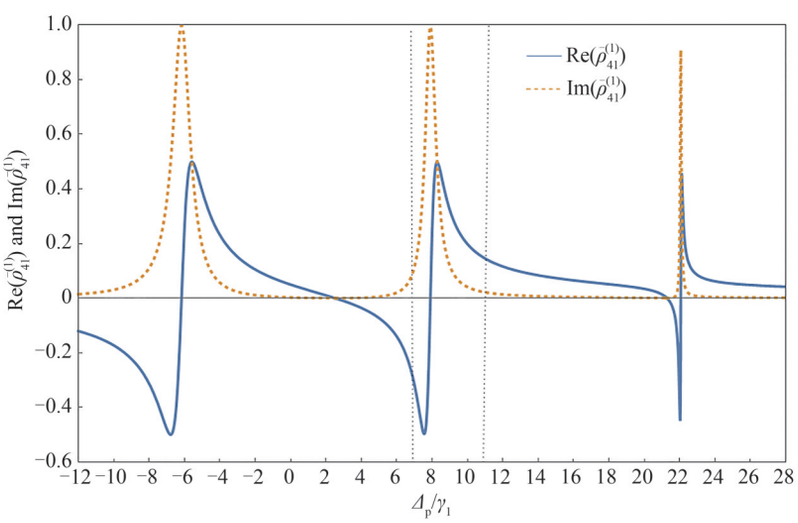

图 3　探测场极化率的折射部分 $\mathrm{Re}\left(\bar{\rho}_{41}^{(1)}\right)$ 和吸收部分 $\mathrm{Im}\left(\bar{\rho}_{41}^{(1)}\right)$ 随失谐 Δ_p 的变化曲线（参数与图 2(b)相同）

Fig. 3　The refractive part $\mathrm{Re}\left(\bar{\rho}_{41}^{(1)}\right)$ and absorptive part $\mathrm{Im}\left(\bar{\rho}_{41}^{(1)}\right)$ of the probe field polarizability versus detuning Δ_p (parameters are the same as in Fig. 2(b))

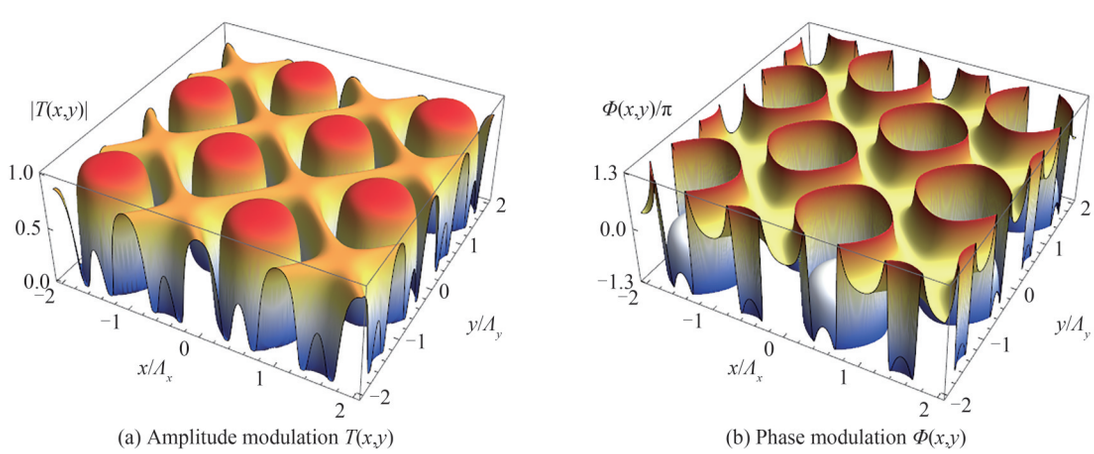

图 4　探测场透射函数的调制图（参数与图 2(b)相同）

Fig. 4　Modulation diagrams of the transmission function of the probe field (parameters are the same as in Fig. 2(b))

为了进一步说明振幅调制和位相调制所起的作用，在图5(a)、(b)中绘制了探测场透射函数振幅调制$\left(\left|T\left(x,y\right)\right|\right)$和位相调制$\mathrm{e}^{\mathrm{i}\Phi(x,y)}$的夫琅禾费衍射图。从图中可以看出，当只有振幅调制存在时，只有一个零级的中心主峰，中心主峰强度约为0.54，基本没有入射光向高阶方向转移；当仅存在位相调制时，零级衍射峰的强度明显减弱，只有0.22左右，而且一级衍射效率得到了提高并达到了6%左右，二级衍射峰的强度也开始显现。另外，其位相调制的衍射强度分布图5(b)与振幅调制和位相调制共同作用时的衍射强度分布图2(b)类似。由此可见，探测场的入射光向高阶方向衍射主要是靠位相调制来完成，而振幅调制对光栅的透射能量有所影响。

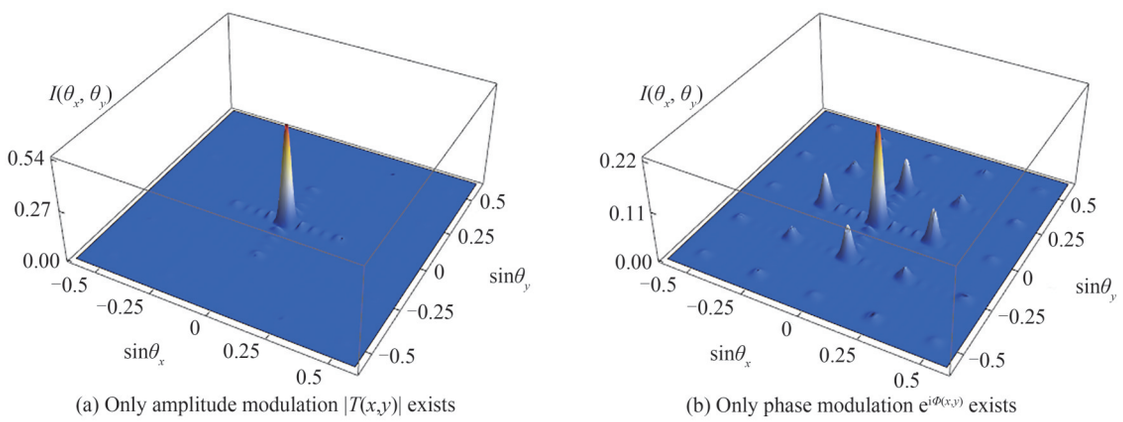

(a) Only amplitude modulation $|T(x,y)|$ exists　　(b) Only phase modulation $\mathrm{e}^{\mathrm{i}\Phi(x,y)}$ exists

图5 夫琅禾费衍射强度随$\sin\theta_x$和$\sin\theta_y$变化分布(参数与图2(b)相同)

Fig. 5 Fraunhofer diffraction intensity as a function of $\sin\theta_x$ and $\sin\theta_y$(parameters are the same as in Fig. 2(b))

探测场失谐量在调节衍射效率方面同样有着重要作用，介质对探测光的吸收依赖于失谐。接下来考察探测场失谐对衍射效率的影响。如图6(a)，继续增加探测场失谐量到$\Delta_\mathrm{p}=11\gamma_1$时，与图2(b)相比，随着失谐量增大，(0,0)级衍射效率$I\left(\theta_x^0,\theta_y^0\right)$从30%降到了11%，而(1,0)或(0,1)级衍射效率$I\left(\theta_x^1,\theta_y^0\right)$或$I\left(\theta_x^0,\theta_y^1\right)$增加到5%，但(1,1)级衍射效率$I\left(\theta_x^1,\theta_y^1\right)$却没有太大变化，仍然是大约1%。究其原因，可以结合图3加以说明：当探测场失谐量Δ_p增加到$11\gamma_1$时，可以发现原子介质对探测场的吸收$\mathrm{Im}\left(\bar{\rho}_{41}^{(1)}\right)$明显减小，同时探测场的色散项$\mathrm{Re}\left(\bar{\rho}_{41}^{(1)}\right)$也相应地减少，在这种情况下，由于振幅调制和位相调制的共同作用，衍射光的一级衍射效率相对于中央级次衍射效率明显增加，二维电磁感应光栅效果越发明显。由此可见，通过调节探测场的失谐，探测场的衍射效率可以得到控制。接下来讨论驻波耦合场强度Ω对光栅衍射图像及衍射效率的影响。由式(3)、(4)和(5)可知，光栅的衍射效率与驻波耦合场强度Ω有关。如图6(b)，在驻波耦合场强度取为

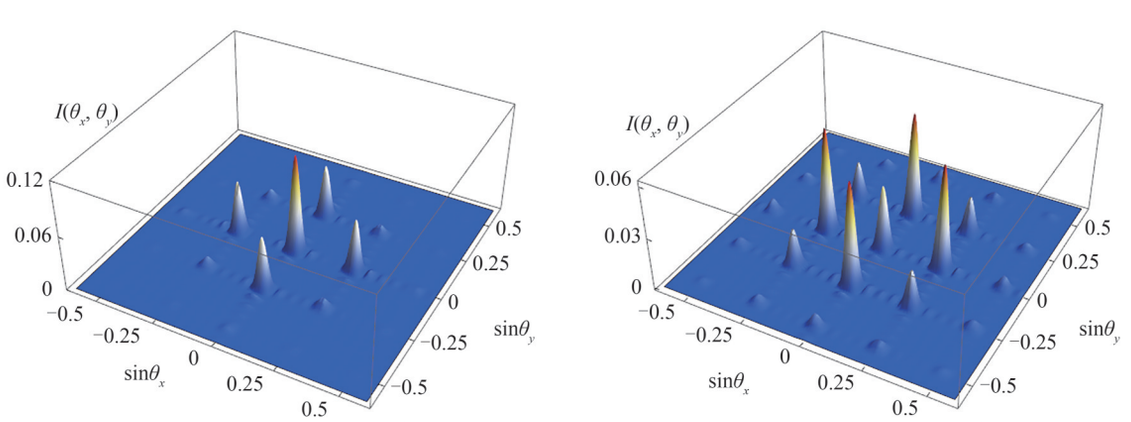

(a) Diffraction pattern of the probe field except for $\Delta_\mathrm{p}=11\gamma_1$ (parameters are the same as in Fig. 2(b))　　(b) Diffraction pattern of the probe field except for $\Omega=10\gamma_1$ (parameters are the same as in Fig. 6(a))

图6 夫琅禾费衍射强度随$\sin\theta_x$和$\sin\theta_y$变化分布

Fig. 6 Fraunhofer diffraction intensity as a function of $\sin\theta_x$ and $\sin\theta_y$

$\Omega=10\gamma_1$时，给出了(0,0)级、(1,0)级、(0,1)级和(1,1)级衍射峰强度的分布图以作说明，与图6(a)相比，当增加驻波耦合场强度时，零级衍射峰强度明由原来的11%显著下降到3.5%，而(1,0)级和(1,1)级衍射峰强度增加到6%，(1,1)级衍射峰强度同样有所增强，达到了2%，而且还有极少量入射光能量向更高阶方向衍射。因此，调节驻波耦合场强度可以在抑制零级衍射峰的同时，提升一级衍射峰的衍射效率，并且对入射光能量向高阶方向转移有所帮助。

通过式(6)可知，光栅的衍射效率与相互作用长度有很大关系，进一步考察相互作用长度L对电磁诱导光栅的衍射效率的影响。图7(a)反映了(0,0)级衍射强度$I\left(\theta_x^0,\theta_y^0\right)$(蓝色实线)、(1,0)级衍射强度$I\left(\theta_x^1,\theta_y^0\right)$(黄色虚线)和(1,1)级衍射强度$I\left(\theta_x^1,\theta_y^1\right)$(绿色虚点线)与相互作用长度$L$的关系。从图中可以看出，当相互作用长度比较小时，探测光能量主要集中在(0,0)级衍射峰，随着相互作用长度的增大，(0,0)级衍射峰强度陡然下降，而(1,0)级和(1,1)级衍射峰开始显现，探测场能量逐渐向高阶方向转移，这是因为相互作用长度增加使得相位调制深度增加，入射光能量逐渐从零级向一级转移。

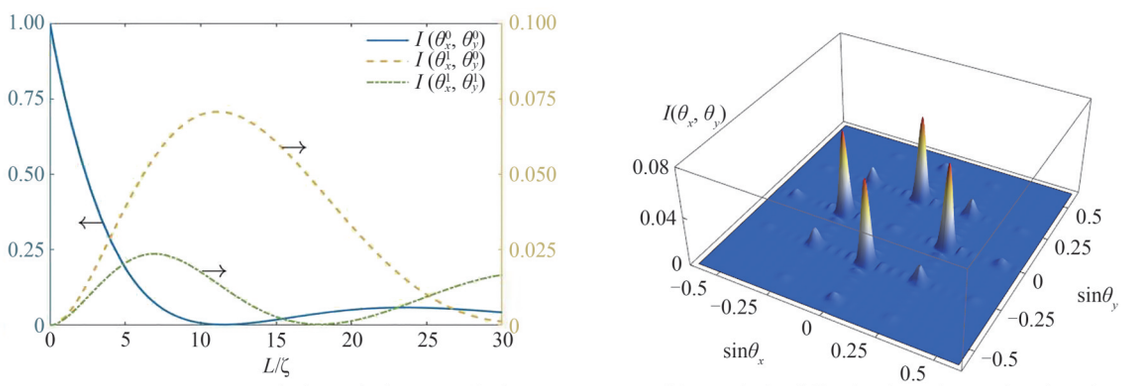

(a) Diffraction intensity $I\left(\theta_x^0,\theta_y^0\right)$, $I\left(\theta_x^1,\theta_y^0\right)$, and $I\left(\theta_x^1,\theta_y^1\right)$ with the interaction length L

(b) Fraunhofer diffraction intensity as a function of $\sin\theta_x$ and $\sin\theta_y$ at the interaction length $L=11\zeta$

图7　相互作用长度L对衍射效率的影响(参数与图6(b)相同)

Fig. 7　Effect of interaction length L on diffraction efficiency(parameters are the same as in Fig.6(b))

当相互作用长度继续增加，位相调制的作用越来越大，(1,0)级和(1,1)级衍射峰强度分别在相互作用长度$L=11\zeta$和$L=7\zeta$时达到最大值，与此同时，(0,0)级衍射峰强度降至为0。但是，随着相互作用长度继续增加，(1,0)级和(1,1)级衍射峰强度又逐渐下降，(0,0)级衍射峰强度又有些许回升。这主要是由于过大的相互作用长度会使介质对探测场的能量的吸收逐渐加大并占据主导地位，导致衍射效率降低。为了更清晰地观察衍射图像，在图7(b)绘制了相互作用长度$L=11\zeta$时探测场的夫琅禾费衍射强度分布图，此时可以看到零级衍射峰强度降至为0，零级衍射峰的能量已经基本衍射到四个一阶衍射峰上，一级衍射效率为7%左右。因此，可以通过有效调节光与原子介质相互作用长度来实现一个高折射率、高衍射效率的二维电磁诱导光栅。

3　结论

本文研究了微波耦合的四能级原子系统的二维电磁感应光栅特性，该原子系统包含一个弱探测场、一个二维驻波耦合场和一个微波场。结果表明，光栅的衍射效率由振幅调制和位相调制共同决定，振幅调制主要影响入射光透过的能量，位相调制主要可以实现将光能量向高阶方向转移。微波场的存在对位相调制有较大影响，对衍射效率的提升大有帮助，通过调节探测场失谐量、驻波耦合场强度以及相互作用长度，可以改变光栅的衍射图像及衍射效率，而且，可以根据实际需要将入射光能量衍射到特定的衍射峰上。本文研究可用于全光分束和光开关，对光信息处理和光网络通信的研究将有所帮助。

参考文献

[1] JYOTSNA I V, AGARWAL G S. Coherent population trapping at low light levels[J]. Physical Review A, 1995, 52(4): 3147.

[2] HARRIS S E, FIELD J E, IMAMOGLU A. Nonlinear optical processes using electromagnetically induced transparency[J]. Physical Review Letters, 1990, 64(10): 1107.
[3] MENON S, AGARWAL G S. Effects of spontaneously generated coherence on the pump-probe response of a Λ system[J]. Physical Review A, 1998, 57(5): 4014.
[4] BROWN A W, XIAO M. All-optical switching and routing based on an electromagnetically induced absorption grating[J]. Optics Letters, 2005, 30(7): 699-701.
[5] ARTONI M, LA ROCCA G C. Optically tunable photonic stop bands in homogeneous absorbing media[J]. Physical Review Letters, 2006, 96(7): 073905.
[6] QIU T H, YANG G J, BIAN Q. Electromagnetically induced second-order Talbot effect[J]. Europhysics Letters, 2013, 101(4): 44004.
[7] CHEN Y Y, LIU Z Z, WAN R G. Beam splitter and router via an incoherent pump-assisted electromagnetically induced blazed grating[J]. Applied Optics, 2017, 56(20): 5736-5744.
[8] LING H Y, LI Y Q, XIAO M. Electromagnetically induced grating: homogeneously broadened medium[J]. Physical Review A, 1998, 57(2): 1338-1344.
[9] TABOSA J W R, LEZAMA A, CARDOSO G C. Transient Bragg diffraction by a transferred population grating: application for cold atoms velocimetry[J]. Optics Communications, 1999, 165(1): 59-64.
[10] BROWN A W, XIAO M. Frequency detuning and power dependence of reflection from an electromagnetically induced absorption grating[J]. Journal of Modern Optics, 2005, 52(16): 2365-2371.
[11] DUTTA B K, MAHAPATRA P K. Electromagnetically induced grating in a three-level Ξ-type system driven by a strong standing wave pump and weak probe fields[J]. Journal of Physics B, 2006, 39(5): 1145.
[12] XIAO Z H, SHIN S G, KIM K. An electromagnetically induced grating by microwave modulation[J]. Journal of Physics B, 2010, 43(16): 161004.
[13] DE ARAUJO L E E. Electromagnetically induced phase grating[J]. Optics Letters, 2010, 35(7): 977-979.
[14] ZHOU F X, QI Y H, SUN H, et al. Electromagnetically induced grating in asymmetric quantum wells via Fano interference[J]. Optics Express, 2013, 21(10): 12249-12259.
[15] XIAO Z H, ZHENG L, LIN H Z. Photoinduced diffraction grating in hybrid artificial molecule[J]. Optics Express, 2012, 20(2): 1219-1229.
[16] CHENG G L, ZHONG W X, CHEN A X. Phonon induced phase grating in quantum dot system[J]. Optics Express, 2015, 23(8): 9870-9880.
[17] GUO Hongju, CHEN Chen, YANG Aihong. Voltage control of electromagnetically induced grating in asymmetric double quantum dot system[J]. Laser & Optoelectronics Progress, 2021, 58(23): 2305001.
郭洪菊, 陈辰, 杨艾红. 不对称双量子点系统中电压调控电磁诱导光栅研究[J]. 激光与光电子学进展, 2021, 58(23): 2305001.
[18] QIU Tianhui, YANG Guojian. Electromagnetically induced grating in a Λ-type three-level atomic system modulated by a microwave field[J]. Acta Physica Sinica, 2012, 61(1): 172-175.
邱田会, 杨国建. 微波射频场调制下Λ型三能级原子系统的电磁感应光栅[J]. 物理学报, 2012, 61(1): 172-175.
[19] YU Song, LIAO Ping, YANG Zhanyu, et al. Electromagnetically induced grating based on the coherent population trapping[J]. Acta Physica Sinica, 2013, 62(22): 224205.
喻松, 廖屏, 杨展予, 等. 基于相干粒子数囚禁的电磁诱导光栅研究[J]. 物理学报, 2013, 62(22): 224205.
[20] NASERI T, SADIGHI-BONABI R. Electromagnetically induced phase grating via population trapping condition in a microwave-driven four-level atomic system[J]. Journal of the Optical Society of America B, 2014, 31(11): 2879-2884.
[21] MA D D, YU D M, ZHAO X D, et al. Unidirectional and controllable higher-order diffraction by a Rydberg electromagnetically induced grating[J]. Physical Review A, 2019, 99(3): 033826.
[22] HANG C, LI W B, HUANG G X. Nonlinear light diffraction by electromagnetically induced gratings with PT symmetry in a Rydberg atomic gas[J]. Physical Review A, 2019, 100(4): 043807.
[23] DONG Yabin, PANG Jialu, YANG Li, et al. Nearly-resonant gain grating in atomic media[J]. Chinese Journal of Lasers, 2021, 48(3): 0312002.
董雅宾, 庞嘉璐, 杨丽, 等. 原子介质中的近共振增益光栅[J]. 中国激光, 2021, 48(3): 0312002.
[24] WANG L, ZHOU F X, HU P D, et al. Two-dimensional electromagnetically induced cross-grating in a four-level tripod-type atomic system[J] Journal of Physics B, 2014, 47(22): 225501.
[25] WU J C, AI B Q. Two-dimensional electromagnetically induced cross-grating in a four-level N-type atomic system[J]. Journal of Physics B, 2015, 48(11): 115504.
[26] CHENG G L, CONG L, CHEN A X. Two-dimensional electromagnetically induced grating via gain and phase modulation in a two-level system[J]. Journal of Physics B, 2016, 49(8): 085501.
[27] CHEN Y Y, LIU Z Z, WAN R G. Two-dimensional electromagnetically induced grating in coherent atomic medium[J].

Europhysics Letters, 2017, 116(6): 64006.
[28] CHEN Y Y, LIU Z Z, WAN R G. Electromagnetically induced two-dimensional grating assisted by incoherent pump[J]. Physics Letter A, 2017, 381(16): 1362-1368.
[29] CHEN Y Y, LIU Z Z, WAN R G. Electromagnetically induced 2D grating via refractive index enhancement in a far-off resonant system[J]. Laser Physics Letters, 2017, 14(7): 075202.
[30] SHUI T, YANG W X, LIU S, et al. Asymmetric diffraction by atomic gratings with optical PT symmetry in the Raman-Nath regime[J]. Physical Review A, 2018, 97(3): 033819.
[31] LIU Y M, GAO F, WU J H, et al. Lopsided diffractions of distinct symmetries in two-dimensional non-Hermitian optical gratings[J]. Physical Review A, 2019, 100(4): 043801.
[32] ARKHIPKIN V G, MYSLIVETS S A. One-and two-dimensional Raman-induced diffraction gratings in atomic media [J]. Physical Review A, 2018, 98(1): 013838.
[33] ASADPOUR S H, KIROVA T, QIAN J, et al. Azimuthal modulation of electromagnetically induced grating using structured light[J]. Scientific Reports, 2021, 11(1): 1-11.
[34] LUKIN M D, YELIN S F, FLEISCHHAUER M, et al. Quantum interference effects induced by interacting dark resonances[J]. Physical Review A, 1999, 60(4): 3225.
[35] NIU Y P, GONG S Q, LI R X, et al. Giant Kerr nonlinearity induced by interacting dark resonances[J]. Optics Letters, 2005, 30(24): 3371-3373.
[36] XIAO Z H, SHIN S G, KIM K. An electromagnetically induced grating by microwave modulation[J]. Journal of Physics B, 2010, 43(16): 161004.
[37] SCULLY M O, ZUBAIRY M S. Quantum optics cambridge university press [M]. Cambridge University Press, Cambridge, 1997.
[38] STECK D A. Rubidium 87 D line data[EB/OL].[2021-09-07].http://steck.us/alkalidata.

Two-dimensional Electromagnetically Induced Grating in Microwave Coupled Four-level Atomic System

XIA Hongming, ZHANG Duo, LI Yaqian, SUN Zhaoyu, WANG Mei
(*School of Electrical and Electronic Engineering, Wuhan Polytechnic University, Wuhan* 430023, *China*)

Abstract: Due to the limitations of traditional gratings, researchers began to look for new methods to fabricate gratings. In recent years, some interesting physical phenomena such as coherent population trapping, electromagnetically induced transparency, spontaneously generated coherence have attracted great attenton. If the standing wave field in the form of spatial modulation is replaced by the traveling wave field in the electromagnetically induced transparency effect, alternating high transmission regions and high absorption regions can be generated. The incident probe light diffracts after passing through the standing wave region, forming a grating-like structure which is named electromagnetically induced grating. Compared with traditional gratings, electromagnetically induced grating shows many advantages. For example, the amplitude and phase can be modulated simultaneously, and the grating constant, diffraction energy and diffraction order can be changed by adjusting the wavelength of the standing wave field, the intensity and detuning of the incident light fields. The concept of electromagnetically induced grating is first proposed theoretically in the three-level Λ-type atomic system. Subsequently, researchers experimentally observe and study the electromagnetically induced grating in cold atomic and hot atomic system successively. In order to improve the diffraction efficiency, more schemes have been proposed to realize electromagnetic induction grating in different atomic system, semiconductor quantum well and quantum dot system, and Rydberg atomic system, etc. In recent years, the research about electromagnetically induced grating has gradually developed to two-dimensional space. By using two orthogonal standing wave fields, two-dimensional electromagnetically induced cross grating can be realized in a tripod four-level atomic system. And some other researchers have then studied the electromagnetically induced grating in different two-level, three-level and four-level atomic system. In addition, P-T symmetry, Raman interaction, azimuth modulation of vortex field also are used to achieve high-efficiency two-dimensional electromagnetically induced grating. Due to its many advantages, electromagnetically induced grating has been applied in the

research fields of photon and optical quantum devices such as all-optical switching and routing, coherent induced photonic band gap, quantum Talbot effect, beam splitting. In this paper, we propose a scheme to study two-dimensional electromagnetically induced grating in a four-level atomic system with double dark states. In our scheme, the microwave field is used to couple two dipole forbidden low-energy levels, and a weak probe field and a two-dimensional standing wave coupling field with periodic spatial intensity are used to drive the transitions between other energy levels, respectively. The Fraunhofer diffraction pattern and diffraction efficiency of the weak probe field are analyzed in the presence or absence of the microwave field. The results show that the existence of microwave field can weaken the zero order diffraction intensity, and significantly increase the first-order diffraction intensity and efficiency. To explain the physical mechanism more clearly, the plot of the refractive index part and the absorption part of the probe field polarizability with the probe detuning is given and disscused in the presence of microwave field. Then, the amplitude modulation and phase modulation are displayed, and the effect of corresponding modulation on Fraunhofer diffraction diagram is analyzed. The results show that the existence of microwave field has great influence on phase modulation. The incident light of the probe field diffracts toward higher order. High-order diffraction is mainly accomplished by phase modulation, but the diffraction energy of the grating controlled by amplitude modulation . At the same time, we discuss the influence of other system parameters, such as the detuning of the probe field, the intensity of the control field and the interaction length on diffraction pattern and diffraction efficiency of the grating in the presence of microwave field. The results show that, by properly tuning the system parameters, the two-dimensional electromagnetically induced grating with high diffraction efficiency can be realized in the system we studied. The scheme proposed can be applied to all-optical beam splitting and optical switching, which is potentially useful for research in optical information processing and optical network communication.

Key words: Electromagnetically induced grating; Microwave field; Phase modulation; Diffraction efficiency; Standing wave laser field

OCIS Codes: 050.1940; 050.1950; 020.1670; 270.1670; 190.2055

Foundation item: National Natural Science Foundation of China (Nos. 11675124, 12105210), Research Project of Wuhan Polytechnic University (No. 2021Y36)